Received: 9 June 2021 | Revised: 9 August 2021 | Accepted: 10 August 2021

DOI: 10.1111/jace.18086

Journal of the American Ceramic Society

ORIGINAL ARTICLE

Rapid synthesis of $Li_4Ti_5O_{12}$ as lithium-ion battery anode by reactive flash sintering

Fangming Liu | **Bin Bai** | **Liang Cheng** | **Chen Xu**

Institute of Materials, China Academy of Engineering Physics, Mianyang, Sichuan, China

Correspondence
Chen Xu, Institute of Materials, China Academy of Engineering Physics, Mianyang, Sichuan 621907 China.
Email: chenxuacademic@163.com

Funding information
National Natural Science Foundation of China, Grant/Award Number: 51702298; Foundation of Sichuan Science and Technology Department, Grant/Award Number: 2018JY0619; Dean Foundation of China Academy of Engineering Physics, Grant/Award Number: YZJJLX2017009; Foundation of Institute of Materials, China Academy of Engineering Physics, Grant/Award Number: TP20160208

Abstract

In this work spinel $Li_4Ti_5O_{12}$ (LTO) was successfully synthesized via flash sintering technique at a furnace temperature of 580°C within only 5 min for the first time. Phase evolution, microstructures, and electrochemical properties were investigated and compared with conventionally synthesized LTO. The flash sintered LTO shows good crystallinity, high purity, and small particle size. More importantly, it suggests that the flash sintering process could help inhibit lithium volatilization and control the particle size, which is vital to the improvement of the lithium-ion diffusion process and battery performance. Compared with the conventionally synthesized samples, the flash sintered LTO exhibits higher specific capacities, better cycling stabilities, and rate capabilities. Therefore, flash sintering shows potentials in improving the electrochemical performance of anode materials, and thus suggests an efficient strategy for rapid synthesis of high-performance anode materials for lithium-ion batteries.

KEYWORDS

anode materials, flash sintering, lithium oxide

1 | INTRODUCTION

Lithium-ion batteries (LIBs) have been dominating the worldwide rechargeable battery market due to their high-energy density, high open circuit voltage, and long lifespan and environmental friendliness.[1,2] In particular, high-energy density LIBs are considered as the ideal power source for electric vehicles (EVs) in the automotive industry. With the rapidly developing market of EVs in recent years, advanced anode materials that possess better safety and cycling stability remains one of the key challenges for LIBs of EV.[3,4] Among existing anode candidate materials, $Li_4Ti_5O_{12}$ (LTO) is a promising alternative to carbon-based materials for LIBs.[5,6] Compared with graphite, LTO has an ultra-flat voltage plateau of 1.55 V versus Li/Li^+, which limits the formation of a solid-electrolyte interface film and hence could avoid the deposition of lithium ions. Meanwhile, the spinel structure of LTO experiences negligible structure change ("zero-strain") during repeated lithium-ion insertion and extraction processes, which could lead to an extremely long cycle life.[7] More importantly, the three-dimensional network channel of the spinel structure gives rapid lithium-ion diffusion, thus excellent lithium-ion insertion/extraction is guaranteed, especially at a high rate. With the advantages above, LTO is regarded as a promising anode for application in high-power and long-life LIBs, especially in EVs.

The conventional synthesis methods of LTO synthesis include solid-state reaction synthesis,[8] sol–gel synthesis,[9] and hydrothermal synthesis,[10] all of which usually undergo an energy-consuming and time-consuming process and take time of more than 10 h at temperature of more than 800°C. Therefore, a fast and energy-saving synthesis route for LTO is needed for large-scale production.

Flash sintering is a high voltage and low current activated sintering technique, which has been developed in

recent years.[11,12] Compared with the conventional method, flash sintering can sinter certain kinds of ceramics in an extremely short time at relatively low furnace temperatures with the assistance of applied electric field. In the past years, this technique has been successfully used in the preparation of a range of ceramic materials, including structural ceramics,[13,14] solid oxide fuel cell materials,[15] ferroelectric materials,[16,17] and composites.[18–20] In our previous work, we successfully applied flash sintering in preparing $LiNi_{1/3}Co_{1/3}Mn_{1/3}O_2$ cathode materials for LIB for the first time, which lowered the synthesis temperature and shortened the holding time of preparing such cathode materials.[21] Considering the relatively long reaction time of preparing anode materials of LIB such as LTO (10 h) via conventional solid-state reaction, it is worth trying to employ flash sintering in the synthesis of LTO.

In this work, we present a rapid and low-temperature synthesis route to prepare spinal LTO by flash sintering for the first time. The phase evolution, morphology, and electrochemical properties of as-prepared LTO anode materials are systematically investigated. The flash sintered LTO exhibits improved capacity, excellent cycling stability, and rate capability, suggesting that flash sintering technique could be a promising method for preparing LIB anode materials.

2 | EXPERIMENTAL METHODS

2.1 | Materials

The raw materials used in the synthesis of LTO are Li_2CO_3 powders (99.9% purity, Aladdin Biochemical Technology Co., Ltd., Shanghai, China) and TiO_2 powders (99.0% purity, Aladdin Biochemical Technology Co., Ltd., Shanghai, China). First, Li_2CO_3 and TiO_2 powders with atom ratio Li/Ti the same as that in formula $Li_4Ti_5O_{12}$ were added into a milling pot, and then ethanol was added. The resultant slurry was ball milled for 12 h, and subsequently dried at 80°C under constant stirring. After drying, the powder mixture was gently ground using an agate mortar, and then pressed into dog-bone-shaped compacts with a gage of 20 mm and a cross section of 2.7 mm × 3.0 mm (Figure S1) by uniaxial pressing at 3 MPa and cold isostatic pressing at 300 MPa. Holes were drilled on each end of the compact samples, and the interior walls of the holes were painted with platinum paste for better electric connection.

2.2 | Refractive flash sintering

The procedure for flash sintering has been described previously.[22] A dog-bone-shaped sample was threaded into platinum wires via the holes, and suspended in a modified furnace (KSL-1400X-A1, Kejing Materials Technology Co., Ltd.). The furnace was heated from room temperature at a rate of 10°C/min until flash sintering occurred. A DC power source (DLM-300, Sorensen) was programmed to apply a constant voltage of 300 V (corresponding to electric field of 150 V/cm), and then was immediately switched to current control when a preset current limit was reached. For holding time experiments of phase evolution, different holding time of 0, 60, 180, 300, and 600 s were set up with a constant current limit of 100 mA. The current was switched off by disconnecting the power at the end of the holding time. The corresponding samples were denoted as FS-0s, FS-60s, FS-180s, FS-300s, and FS-600s, respectively. For the current limit experiments, different current limits of 60, 80, 100, 120, 140, and 160 mA were set up with a constant holding time of 300 s. The corresponding samples were denoted as FS-60mA, FS-80mA, FS-100mA, FS-120mA, FS-140mA, and FS-160mA, respectively, with corresponding current densities of 7.47, 9.96, 12.45, 14.94, 17.43, and 19.92 mA/mm^2, respectively. After the power disconnection, the sample was cooled down to room temperature at 5°C/min with furnace. For comparison, two samples were also prepared via conventional solid-state reaction by calcination of a same compact at 850°C for 12 h in the same furnace: one sample was prepared by raw materials with theoretical ratio (denoted as CS-a) and the other one with 5 mol% excess of Li (denoted as CS-b), respectively.

2.3 | Characterization

Powders for characterization were ground from gage sections of sintered samples. The phase structure of these as-prepared samples was examined by X-ray diffraction (XRD, Rigaku D/max-2400, Tokyo, Japan) using Cu Kα radiation. The morphology of these samples was observed by scanning electron microscope (SEM, EM5000, KYKY, China).

2.4 | Electrochemical measurements

The electrochemical performance of the as-prepared LTO materials was systematically examined in CR2032 coin-type cells. The slurry that includes active materials, super P, and polyvinylidene fluoride (PVDF, dissolved in *N*-methyl-2-pyrrolidinone) with a weight ratio of 8:1:1 was coated on copper foil to present the LTO electrode. Then the electrode was dried at 120°C for 10 h in a vacuum oven. Metallic lithium foil was used as the counter electrode. The solution of 1 M $LiPF_6$ in

ethylene carbonate, dimethyl carbonate, and ethyl methyl carbonate with a volume ratio of 1:1:1 was used as the electrolyte. The Celgard 2400 polyethylene film was used as the separator. Half cells were assembled in an argon-filled glovebox.

The galvanostatic charge/discharge tests at different current densities were conducted between 1.0 V and 2.5 V on a Land CT2001A battery test instrument (Wuhan Jinnuo Electronics Co., Ltd.) at room temperature. The electrochemical impedance spectra (EIS) were measured on a CHI760E electrochemical workstation (CH Instruments, Inc.) in a frequency range of 10^{-2} Hz to 10^{5} Hz.

3 | RESULTS AND DISCUSSION

The power dissipation spike under a constant applied voltage of 300 V at the furnace temperature of around 580°C in Figure 1A along with a corresponding densification in Figure 2 indicate that the precursor powder mixture of LTO was flash sintered. The holding time of 0 s in Figure 1A,B represents the time when the current reaches the preset current limit. The voltage undergoes a drop from 300 V to a current control state at the onset of flash sintering, and then varies automatically to maintain the current at the value of preset current limit, as shown in Figure 1B.

The shrinkage strain as a function of holding time of samples subjected to applied voltage of 300 V and current of 100 mA is shown in Figure 2. Here, the shrinkage strain ε is given by the following equation:

$$\varepsilon = \ln\frac{l}{l_0} \tag{1}$$

where l_0 is the initial gage length and l is the time-dependent gage length during flash sintering process. The whole flash sintering process is distinctly divided into three stages: An incubation stage before the onset of flash sintering (Stage I), which is seen as field-assisted sintering (FAS), a sharp shrinkage that occurs in the initial few seconds of flash sintering (Stage II), followed by an temperature-steady stage driven by the "I^2R" Joule heating (Stage III) which is also seen as an FAS process.[23,24] Stage III is a special state achieved during the flash sintering process, where the temperature attains a steady state and sample shrinks gradually as holding time lasts. This is consistent with our previous work.[22] Therefore, the sintering technique used here could be accurately named as "flash/field-assisted sintering," which is a hybrid of flash sintering and FAS.

In order to investigate the influence of holding time and current density on the phase evolution, samples were flash sintered under different holding time and current limits. In addition, the conventional solid-state reaction method was also employed to prepare LTO for comparison. Figure 3A shows the XRD patterns of conventionally synthesized sample and flash sintered samples with different holding time. According to the XRD patterns, sample CS-a, FS-0s, FS-60s, FS-180s, FS-300s, and FS-600s all are typically indexed to cubic LTO (JCPDS 49-0207). In the XRD pattern of the conventionally synthesized sample CS-a, very weak peaks at 2θ of 27.4° and 54.3° are observed, which correspond to the residue of rutile TiO_2. This is because a long time duration of 12 h and a high reaction temperature of 850°C is applied in the conventional solid-state reaction method to prepare CS-a sample, which could lead to the volatilization of lithium, leaving a small amount of anatase TiO_2 unreacted. Therefore, the rutile TiO_2 residue is

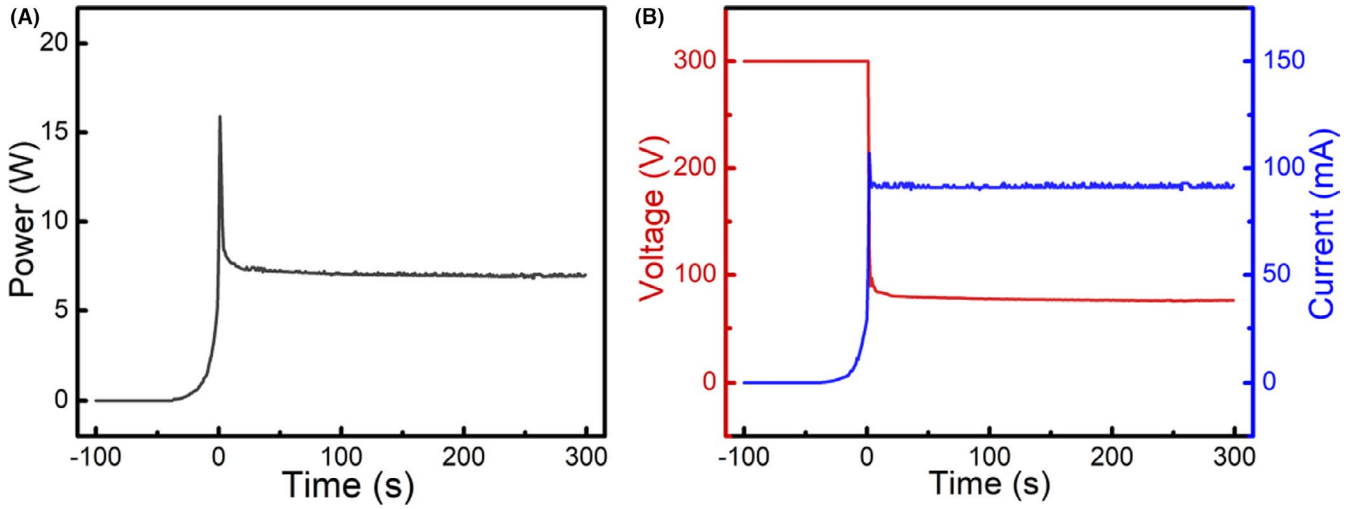

FIGURE 1 Time dependence of (A) power dissipation, (B) applied voltage and current of sample FS-100 mA during the flash sintering process

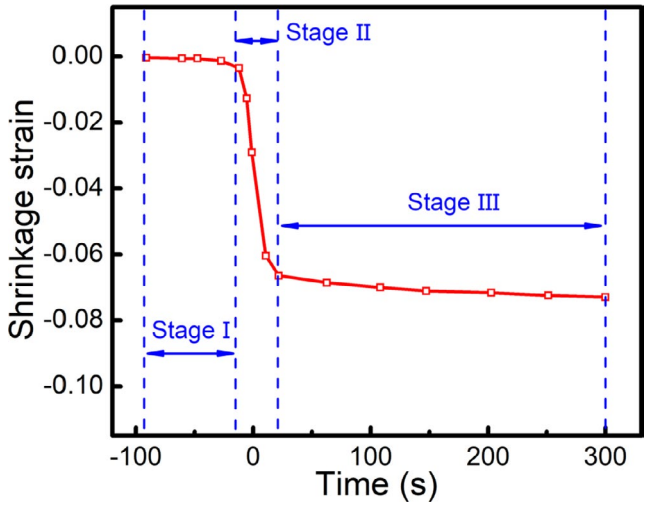

FIGURE 2 Shrinkage versus time during flash sintering process under 300 V and 100 mA

formed from the unreacted anatase TiO_2 during the formation of LTO. In the XRD pattern of FS-0s, the phase of LTO already appears along with anatase TiO_2 at the start of flash sintering (holding time of 0 s), which indicates that accelerated diffusion occurs at the instant of flash sintering, and the reaction between reactants occurs concurrently. The existence of anatase TiO_2 phase in sample FS-0s also indicates that the synthesis reaction of LTO has not been completely finished at the start of flash sintering. With holding time of 60 s, the diffraction peaks of FS-60s match quite well with the standard pattern without obvious peaks of second phase, indicating that a pure phase of LTO can be obtained within 1 minute by flash sintering, from raw materials with atom ratio Li/Ti the same as that in formula $Li_4Ti_5O_{12}$. This could be because the lithium volatilization is inhibited within such short time duration in the flash sintering process, which will contribute to a better battery performance. With extended holding time, the intensity of LTO phase peaks increases gradually, and meanwhile, the peak splitting at (400) and (440) becomes more clear, indicating that the crystallinity of LTO is increased. XRD results also show that the crystallite size increases as the holding time lasts, which is calculated according to Scherrer equation (see Table S1). Whereas almost no change is found between the patterns of FS-300s and FS-600s, indicating that the further extension of holding time has little influence on the crystallinity of LTO.

Although flash sintering of LTO occurred at the furnace temperature of 580°C, the sample temperature could be much higher due to Joule heating.[24–26] Therefore, samples were flash sintered under different current limits to study the influence of Joule heating on LTO synthesis. Figure 3B shows that the XRD patterns of samples flash sintered at different current limits. At low current of 60 mA, TiO_2 still exists in the flash sintered samples. At current of 80, 100, and 120 mA, no obvious impurity can be found. When increasing the current to 140 mA, significant impurity peaks are found and assigned to Li_2TiO_3 and $Li_2Ti_3O_7$, which could be the decomposition products of LTO at high temperature. With further increasing the current up to 160 mA, the decomposition products become a major component of the sample. According to literature,[27] the decomposition of LTO is mainly ascribed to the high temperature (above 1015°C) of the samples, which are significantly higher than the furnace temperature (580°C). Therefore, it can be speculated that Joule heating caused by flash sintering is responsible for the decomposition of LTO. The sample temperature is estimated by using black body radiation model,[23,24,26] in which the Stefan–Boltzmann law is employed in the form of the following equation:

$$\frac{T^*}{T_F} = \left[1 + \frac{1000 \cdot W_V}{e_m \sigma T_F^4}\left(\frac{V}{A}\right)\right]^{\frac{1}{4}} \quad (2)$$

where T^* and T_F are the temperature of the sample and the furnace, respectively, W_V is the electrical energy expended in the sample, e_m is the emissivity, σ is Stefan–Boltzmann constant ($\sigma = 5.67 \times 10^{-8}$ W m^{-2} K^{-4}), and the ratio of the volume divided by the surface area of the sample is written as (V/A). The parameters of the samples and the calculated sample temperature are presented in the Table S2. Based on calculation, the real sample temperature of sample FS-60mA is 716°C, which cannot provide enough energy for diffusion in short time, with unreacted components TiO_2 phase left from the synthesis process. In comparison, the temperature of sample FS-140mA and FS-160mA is calculated to be 909 and 964°C, which is close to the decomposition temperature of 1050°C, resulting in partial decomposition of LTO. On the whole, sharp diffraction peaks of LTO phase are exhibited in the XRD patterns of flash sintered samples at current of 80, 100, and 120 mA, suggesting that LTO of good crystallinity and high purity could be prepared by flash sintering, a fast and energy-saving way, at a reduced temperature of 580°C and a shortened reaction time of 5 min.

A pure LTO sample CS-b (see Figure 3B) via conventional method was also prepared. The morphology of the conventionally synthesized and flash sintered samples is shown in Figure 4. It can be seen that the LTO powder CS-b prepared by conventional solid-state reaction method has particle size of about 900 ± 400 nm (Figure 4A). In the case of the flash sintered samples, it is observed that the particle size increases with increasing the current limit. FS-80mA, FS-100mA, and FS-120mA show particle size of about 350 ± 150, 400 ± 150, and 550 ± 200 nm, respectively

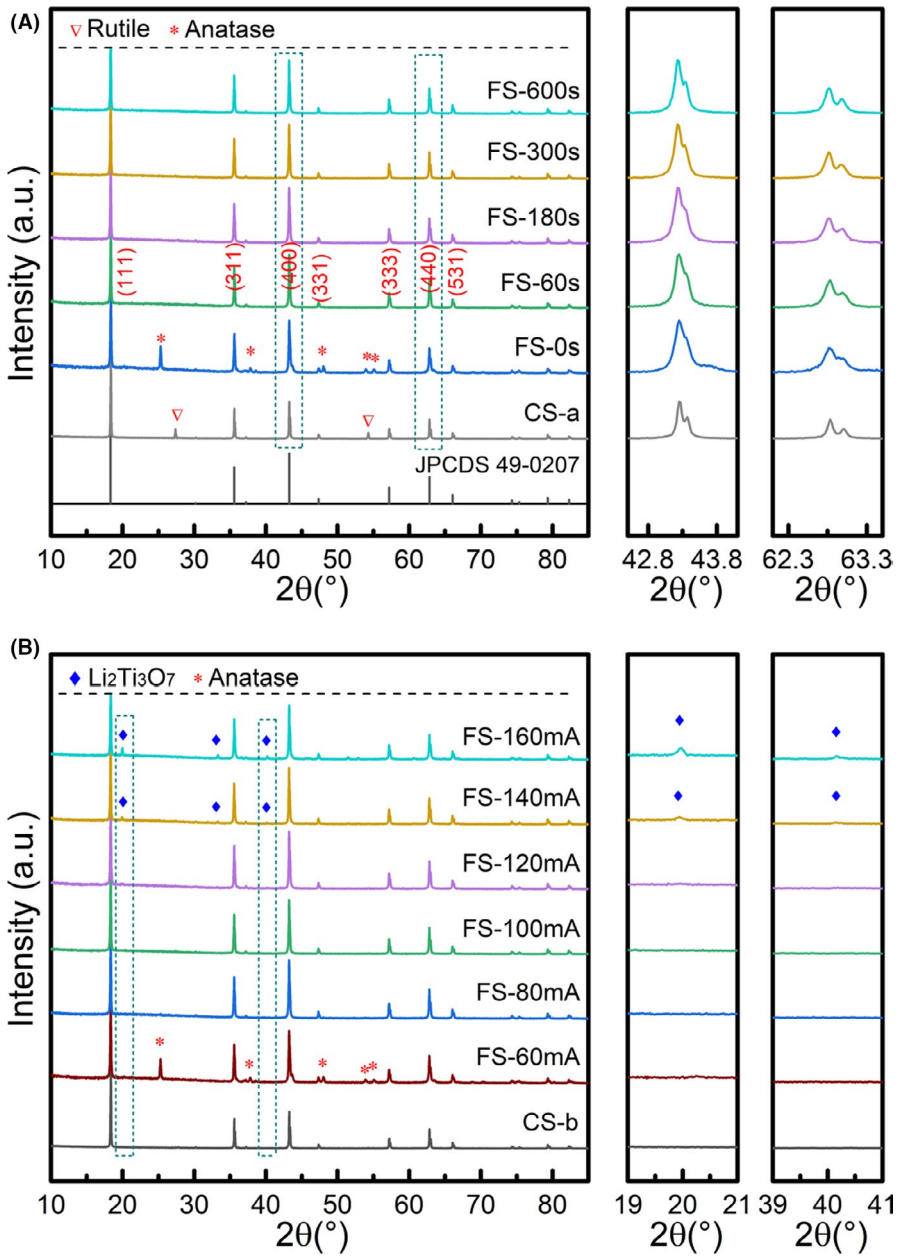

FIGURE 3 XRD patterns of (A) samples prepared by conventional solid-state reaction and samples flash sintered at 100 mA with different holding time, and (B) samples flash sintered with different current limits

(Figure 4B–D), which are obviously smaller than that of conventionally synthesized LTO. This phenomenon can be explained by the short sintering duration in flash sintering process, which restricts particle growth of LTO. And the particle size can be adjusted by controlling the current limit during the flash sintering process.

The electrochemical performance of the conventionally synthesized and flash sintered samples was systematically examined in CR2032 coin-type cells. All samples exhibit obvious charge/discharge plateau at 2.5–1.0 V, which corresponds to the lithium-ion insertion and extraction process in the spinal LTO. The initial discharge capacity of FS-80mA, FS-100mA, and FS-120mA is 163.7, 164.9, and 161.9 mAh/g, respectively. In comparison, sample CS-b delivers an initial discharge capacity of only 156.3 mAh/g. One can see that the flash sintered samples exhibit higher initial discharge capacity than the conventionally synthesized sample. The improved capacity of the flash sintered samples can be explained by a higher crystallinity and a relatively smaller particle size due to flash sintering process.[28]

The cycling performance of these samples at rate of 1C (175 mA/g) was tested, as shown in Figure 5B. Sample CS-b achieves a capacity retention of 92.7% after 50 cycles at rate of 1C. In the case of the flash sintered samples, FS-80mA, FS-100mA, and FS-120mA show the capacity retention of 95.0%, 94.9%, and 93.2% after 50 cycles at rate of 1C, respectively. It can be seen that all the flash sintered samples possess higher discharge capacity and better cycling stability than that of CS-b. Especially, FS-80mA is verified to have the best cycling performance. It can be speculated that the improved capacity retention for flash

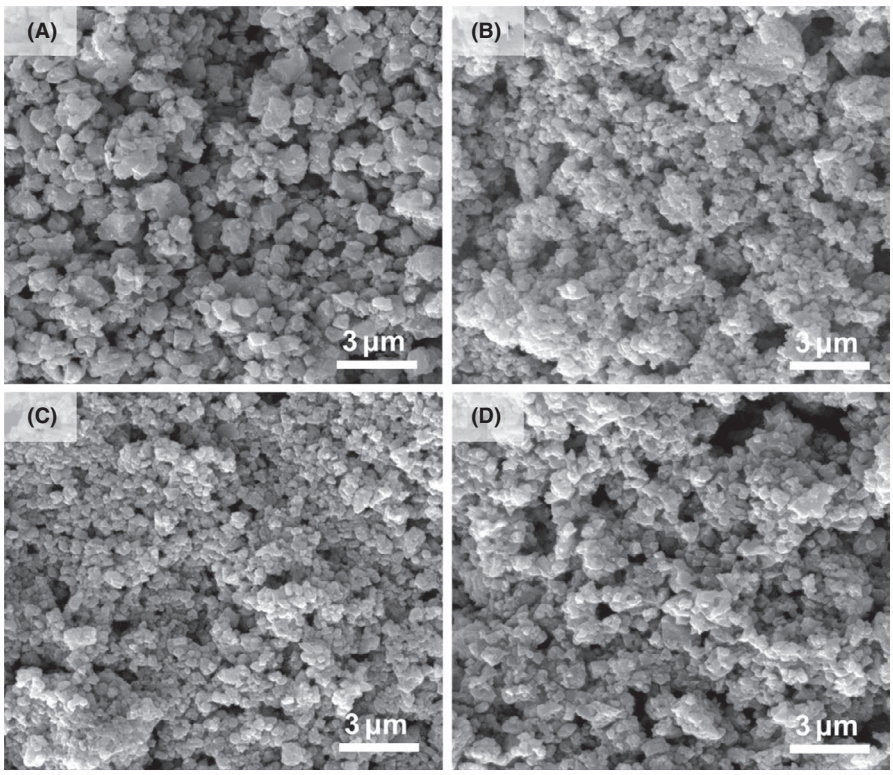

FIGURE 4 SEM images of LTO powders of sample (A) CS-b, (B) FS-80mA, (C) FS-100mA, and (D) FS-120mA

sintered samples might be related to the enhanced ionic conductivity resulted from flash sintering.

The rate capacity at different rates of 1, 2, 5, 10, and 20 C (1C = 175 mA/g) are shown in Figure 5C. It can be seen that the rate capacity of flash sintered sample FS-80mA and FS-100mA is significantly improved in comparison to CS-b. The capacity of CS-b seriously decreases as the current rate is raised. Sample FS-120mA shows a quite similar performance with that of CS-b. Whereas the flash sintered samples FS-80mA and FS-100mA exhibit less capacity degradation. Specifically, sample CS-b has a discharge capacity of 156.3, 135.1, 113.2, 89.8, and 67.3 mAh/g at 1, 2, 5, 10, and 20 C, respectively. In comparison, the corresponding discharge capacities of FS-80mA are 163.6, 152.4, 145.4, 136.0, and 118.7 mAh/g, respectively, with improvement of 4.67%, 12.8%, 28.4%, 51.4%, and 76.4%. One can see that flash sintering significantly improves the cycling stability and the rate capability of LTO. It is possible the short time duration in the flash sintering process inhibits the amount of lithium volatilization, especially for the surface of LTO particle, leading to more lithium ion charge carriers available for transport at the particle surface, which is good for the diffusion process of lithium ions. In addition, a relative smaller particle size achieved by flash sintering will enhance the active surface area and shorten the lithium-ion transfer path, which contribute to the diffusion process and electrode reaction kinetics.

The kinetic behavior of these samples was further investigated using EIS. As shown in Figure 5D, all the samples exhibit EIS spectra consisting of a semicircle at high frequency and a slope line at low frequency. Specifically, the slope line in the low-frequency represents Warburg impedance (Z_w), which reflects the lithium-ion diffusion resistance within the anode. The semicircle at high frequency refers to the charge-transfer resistance (R_{ct}) at the electrode–electrolyte interface, and the intersection of the semicircle with the real axis at high frequency corresponds to the solution resistance (R_s). The EIS spectra were modeled using equivalent circuit (Scheme S1) fitting in ZView® software, and the corresponding fitted parameters are obtained in Table 1. The simulated R_{ct} of sample CS-b, FS-80mA, FS-100mA, and FS-120mA are 71.4, 36.2, 54.7, and 75.7 Ω, respectively. One can see that the R_{ct} of the flash sintered samples FS-80mA and FS-100mA are much smaller than that of the conventionally synthesized sample, and sample FS-80mA is verified to have the smallest value. In addition, the lithium diffusion coefficient (D_{Li}) can be calculated by the following equation[29]:

$$D_{Li} = \frac{R^2T^2}{2A^2n^4F^4C_{Li}^2\sigma^2} \tag{3}$$

$$Z' = R_s + R_{ct} + \sigma\omega^{-\frac{1}{2}} \tag{4}$$

where R is the gas constant, T the temperature, A the surface area, n the number of electrons per molecule participating in the electron-transfer reaction, F the Faraday

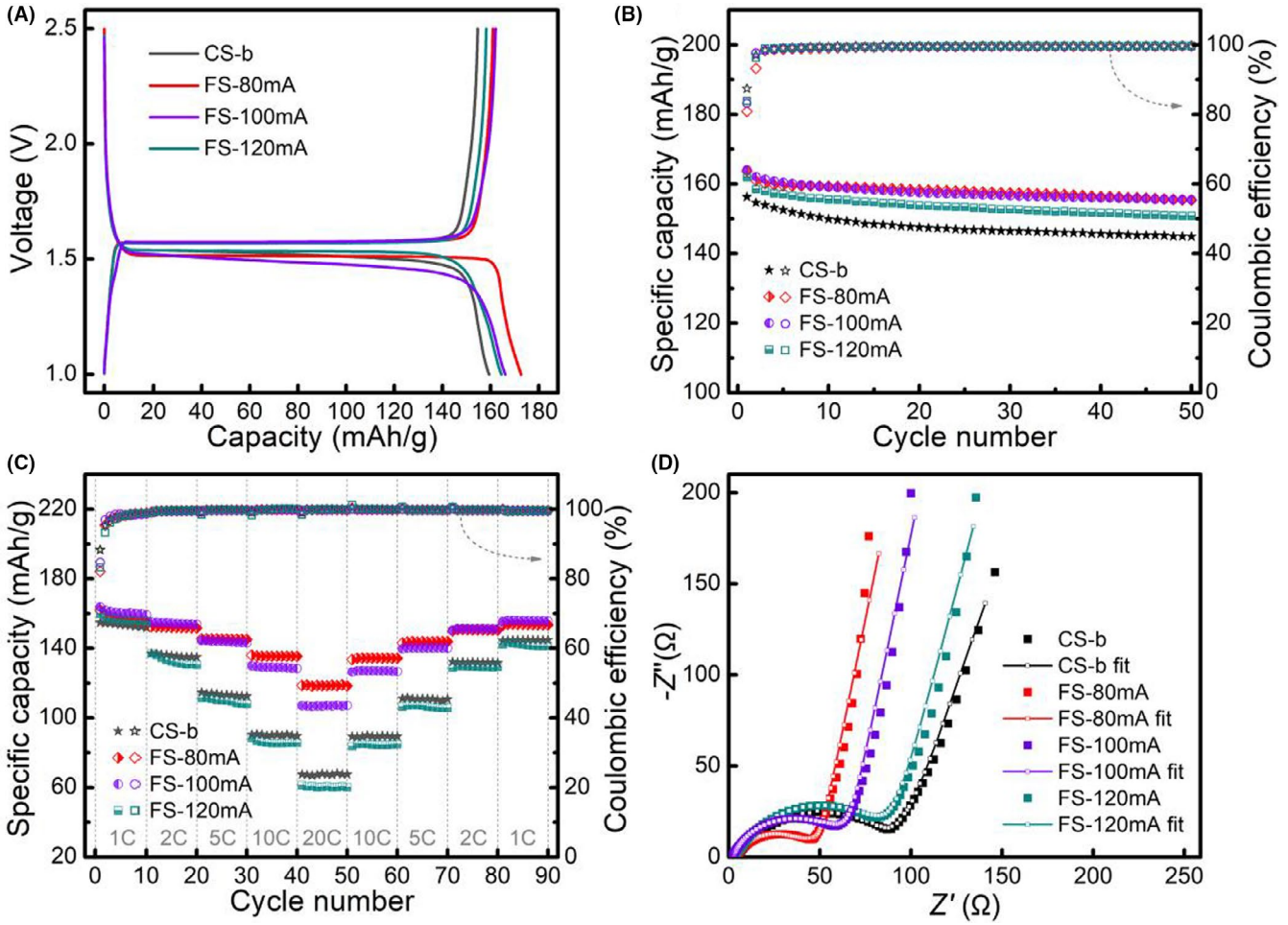

FIGURE 5 Electrochemical performances of the as-prepared LTO: (A) the initial discharge–charge curves at 0.1 C, (B) the discharge cycling performances at 1 C, (C) the rate capabilities at different rates, (D) the experimental and simulated EIS spectra

TABLE 1 Parameters of EIS for the as-prepared LTO electrodes

Samples	R_s (Ω)	R_{ct} (Ω)	σ (Ω cm^2 $s^{-0.5}$)	D_{Li} (cm^2 s^{-1})
CS-b	5.06	71.4	86.5	8.82×10^{-13}
FS-80mA	4.50	36.2	50.8	2.56×10^{-12}
FS-100mA	2.05	54.7	60.5	1.80×10^{-12}
FS-120mA	4.98	75.7	78.5	1.07×10^{-12}

constant, C_{Li} the concentration of lithium-ion, ω the angular frequency, and σ the Warburg factor. From equation 4, the Z' as a function of $\omega^{-1/2}$ was plotted (Figure S2), and the slope σ can be obtained and then used in equation 3. The lithium diffusion coefficients of sample CS-b, FS-80mA, FS-100mA, and FS-120mA are calculated to be 8.82×10^{-13}, 2.56×10^{-12}, 1.80×10^{-12}, and 1.07×10^{-12} cm^2/s, respectively. One can see that lithium diffusion coefficients of the flash sintered samples are larger than that of the conventionally synthesized sample, and sample FS-80mA is verified to have the largest value. It can be certified that a reduced charge-transfer resistance and increased lithium diffusion coefficient is beneficial to the kinetic behaviors during the charge/discharge process. The EIS results prove that flash sintering is effective in improving the conductivity of LTO, and then improves the rate performance. This agrees well with the results of rate capability experiment. It is inferred that the improved lithium-ion diffusion process is benefitted from the reduced particle size and the inhibited of lithium volatilization, which can be seen as advantages for the flash sintering technique.

4 | CONCLUSION

In summary, this work demonstrates for the first time that spinal LTO was successfully synthesized within a few minutes at a low furnace temperature of 580°C by using flash sintering technique. Lithium volatilization is inhibited in the flash sintering process, resulting in the LTO product with good crystallinity and

high purity. The morphology analysis reveals that the flash sintered samples exhibit reduced and controllable particle size, which can be realized by adjusting the current limit during flash sintering process. Compared with the conventionally synthesized sample, the flash sintered LTO exhibits higher specific capacities, better cycling stabilities, and rate capabilities. It is proposed that the inhibited lithium volatilization and reduced particle size are responsible for the improved lithium-ion diffusion process, and thus leads to enhanced performance of LTO. Therefore, the flash sintering technique has presented its potentials in the improvement of LTO performance, which provides a novel strategy for fast synthesis of high-performance anode materials for lithium-ion batteries.

ACKNOWLEDGMENTS

This work was financially supported by the National Natural Science Foundation of China (No. 51702298), the Foundation of Sichuan Science and Technology Department (No. 2018JY0619), the Dean Foundation of China Academy of Engineering Physics (No. YZJJLX2017009), and Foundation of Institute of Materials, China Academy of Engineering Physics (TP20160208).

ORCID

Chen Xu https://orcid.org/0000-0002-1359-4923

REFERENCES

1. Wu FX, Maier J, Yu Y. Guidelines and trends for next-generation rechargeable lithium and lithium-ion batteries. Chem Soc Rev. 2020;49(5):1569–614.
2. Fan ES, Li L, Wang ZP, Lin J, Huang YX, Yao Y, et al. Sustainable recycling technology for Li-ion batteries and beyond: challenges and future prospects. Chem Rev. 2020;120(14):7020–63.
3. Zeng XQ, Li M, Abd El-Hady D, Alshitari W, Al-Bogami AS, Lu J, et al. Commercialization of lithium battery technologies for electric vehicles. Adv Energy Mater. 2019;9(27):1900161.
4. Ding YL, Cano ZP, Yu AP, Lu J, Chen ZW. Automotive Li-ion batteries: current status and future perspectives. Electrochem Energ Rev. 2019;2(1):1–28.
5. Yan H, Zhang D, Qilu DX, Sheng XL. A review of spinel lithium titanate ($Li_4Ti_5O_{12}$) as electrode material for advanced energy storage devices. Ceram Int. 2021;47(5):5870–95.
6. Yuan T, Tan ZP, Ma CR, Yang JH, Ma ZF, Zheng SY. Challenges of spinel $Li_4Ti_5O_{12}$ for lithium-ion battery industrial applications. Adv Energy Mater. 2017;7(12):25.
7. Ohzuku T, Ueda A, Yamamoto N. Zero-strain insertion material of $Li[Li_{1/3}Ti_{5/3}]O_4$ for rechargeable lithium cells. J Electrochem Soc. 1995;142(5):1431–5.
8. Li DL, Zhang XX, Miao XF, Liu YC, Chen SJ, Chen YQ, et al. Solid-state synthesized $Li_4Ti_5O_{12}$ for ultrafast lithium ion storage enabled by carbon-coating induced particle size tailoring. J Alloy Compd. 2019;797:1258–67.
9. Zhang L, Zhang JD, Luo X, Long YF, Xue X, Yin Y, et al. Electrochemical performance of $Li_4Ti_5O_{12}$ anode material synthesised using polyethylene glycol as a template agent. Ceram Int. 2021;47(4):4729–36.
10. Zhang EW, Zhang HL. Hydrothermal synthesis of $Li_4Ti_5O_{12}$-TiO_2 composites and $Li_4Ti_5O_{12}$ and their applications in lithium-ion batteries. Ceram Int. 2019;45(6):7419–26.
11. Cologna M, Prette ALG, Raj R. Flash-sintering of cubic yttria-stabilized zirconia at 750°C for possible use in SOFC manufacturing. J Am Ceram Soc. 2011;94(2):316–9.
12. Yu M, Grasso S, McKinnon R, Saunders T, Reece MJ. Review of flash sintering: materials, mechanisms and modelling. Adv Appl Ceram. 2017;116(1):24–60.
13. Martinez JM, Biesuz M, Dong J, Gauna M, Srez G, Sglavo VM, et al. Flash sintering of zircon: rapid consolidation of an ultra-high bandgap ceramic. J Asian Ceram Soc. 2021;9(1):374–81.
14. Biesuz M, Sglavo VM. Flash sintering of alumina: effect of different operating conditions on densification. J Eur Ceram Soc. 2016;36(10):2535–42.
15. Zhang J, Zhao YT, Qiao JS, Sun W, Sun KN, Wang ZH. An easily controllable flash sintering process for densification of electrolyte for application in solid oxide fuel cells. Int J Hydrogen Energy. 2020;45(35):17824–32.
16. Liu J, Ren K, Ma CY, Du HL, Wang YG. Dielectric and energy storage properties of flash-sintered high-entropy $(Bi_{0.2}Na_{0.2}K_{0.2}Ba_{0.2}Ca_{0.2})TiO_3$ ceramic. Ceram Int. 2020;46(12):20576–81.
17. Taghaddos E, Charalambous H, Tsakalakos T, Safari A. Electromechanical properties of flash sintered BNT-based piezoelectric ceramic. J Eur Ceram Soc. 2019;39(9):2882–8.
18. Ojaimi CL, Ferreira JA, Chinelatto AL, Chinelatto ASA, Pallone E. Microstructural analysis of ZrO_2/Al_2O_3 composite: flash and conventional sintering. Ceram Int. 2020;46(2):2473–80.
19. Jia YJ, Su XH, Wu YJ, Wang ZJ, Meng LC, Xu XQ, et al. Flash sintering of 3YSZ/Al_2O_3-platelet composites. J Am Ceram Soc. 2020;103(4):2351–61.
20. Fele G, Biesuz M, Bettotti P, Moreno R, Sglavo VM. Flash sintering of yttria-stabilized zirconia/graphene nano-platelets composite. Ceram Int. 2020;46(14):23266–70.
21. Shi PR, Qu GX, Cai SK, Kang YJ, Fa T, Xu C. An ultrafast synthesis method of $LiNi_{1/3}Co_{1/3}Mn_{1/3}O_2$ cathodes by flash/field-assisted sintering. J Am Ceram Soc. 2018;101(9):4076–83.
22. Xu C, Wang LX, Bai B, Peng L, Cai SK. Rapid synthesis of $Gd_2Zr_2O_7$ ceramics by flash sintering and its aqueous durability. J Eur Ceram Soc. 2020;40(4):1620–5.
23. Chaim R. Insights into photoemission origins of flash sintering of ceramics. Scripta Mater. 2021;196.
24. Raj R. Joule heating during flash-sintering. J Eur Ceram Soc. 2012;32(10):2293–301.
25. Zhu FX, Peng XY, Liu JL, Liu DG, Ren K, Wang YG. Surface temperature distribution on dense 8YSZ ceramics during the steady stage in AC flash sintering. Ceram Int. 2021;47(2):2884–7.

26. Biesuz M, Luchi P, Quaranta A, Martucci A, Sglavo VM. Photoemission during flash sintering: an interpretation based on thermal radiation. J Eur Ceram Soc. 2017;37(9):3125–30.
27. Mergos JA, Dervos CT. Structural and dielectric properties of Li_2O-doped TiO_2. Mater Charact. 2009;60(8):848–57.
28. Yang ZG, Choi D, Kerisit S, Rosso KM, Wang DH, Zhang J, et al. Nanostructures and lithium electrochemical reactivity of lithium titanites and titanium oxides: a review. J Power Sources. 2009;192(2):588–98.
29. Yi TF, Xie Y, Wu QJ, Liu HP, Jiang LJ, Ye MF, et al. High rate cycling performance of lanthanum-modified $Li_4Ti_5O_{12}$ anode materials for lithium-ion batteries. J Power Sources. 2012;214:220–6.

SUPPORTING INFORMATION

Additional supporting information may be found online in the Supporting Information section.

How to cite this article: Liu F, Bai B, Cheng L, Xu C. Rapid synthesis of $Li_4Ti_5O_{12}$ as lithium-ion battery anode by reactive flash sintering. J Am Ceram Soc. 2022;105:419–427. https://doi.org/10.1111/jace.18086